SUPPORTING INFORMATION

AUTHORS

Miguel A. Ruiz-Fresneda, Margarita Lopez-Fernandez, Marcos F. Martinez-Moreno, Andrea Cherkouk, Yon Ju-Nam, Jesus J. Ojeda, Henry Moll, Mohamed L. Merroun

TITLE

Molecular binding of Eu^{III}/Cm^{III} by S*tenotrophomonas bentonitica* and its impact on the safety of future geodisposal of radioactive waste

NUMBER OF PAGES: 16

NUMBER OF FIGURES: 4

NUMBER OF TABLES: 3

1. Supplementary materials and methods

1.1. Preparation of Eu^{III} and Cm^{III} stock solutions

A stock solution of Eu^{III} was prepared by dissolving europium chloride ($EuCl_3 \cdot 6H_2O$) (Sigma-Aldrich) in 0.1 M HCl to a final concentration of 10 mM. For the experiments, an Eu^{III} working solution was prepared diluting the stock in 0.1 M $NaClO_4$ to a final concentration of 30 μM. Analytical grade 0.1 M $NaClO_4$ (Merck, Darmstadt, Germany) was used as a background electrolyte. On the other hand, a stock solution of the long-lived Cm isotope ^{248}Cm (half-life: 3.4×10^5 years) was used as described in Lopez-Fernandez et al.[1] This solution had the following composition: 97.3% ^{248}Cm, 2.6% ^{246}Cm, 0.04% ^{245}Cm, 0.02% ^{247}Cm, and 0.009% ^{244}Cm in 1 M $HClO_4$. To prevent the carbonate complexation of Cm^{III} carbonate-free water and NaOH solution were used. The pH of the solutions was adjusted by addition of small volumes of acid ($HClO_4$) or base (NaOH) using an InLab Solids combination pH puncture electrode (Mettler-Toledo, Giessen, Germany) and sterilized by filtration through 0.22 μm nitrocellulose filters. In the case of anaerobic experiments, the solution was degassed with N_2 prior its use in a glove box under a N_2 atmosphere at 25 °C.

1.2. Potentiometric titration of cell surfaces of *S. bentonitica* treated with Eu^{III}

Potentiometric titrations were carried out to characterize the chemistry of *S. bentonitica* surfaces in presence of Eu^{III} under aerobic conditions. All titrations were performed using a Metrohm Titrando 906 automatic titrator (Metrohm, UK) at 25 ºC. The temperature was kept constant and continuously monitored during the titration. The titrator was set to add successive acid or base only after a drift equal or less than 5 mV/min was achieved.

An amount of *S. bentonitica* equivalent to 0.4 g/L of dry biomass, previously washed four times with 0.1 M $NaClO_4$, was suspended in a vessel with 25 mL CO_2-free 0.1 M $NaClO_4$ solution containing 30 µM Eu^{III}. Bacterial samples suspended in 0.1 M $NaClO_4$ were employed as control. The suspension was titrated with 0.1 M HCl to pH 3.5 and then with 0.1 M NaOH to pH 10.0. To test the reversibility of the protonation-deprotonation behavior, the suspension was back-titrated with 0.1 M HCl from pH 10.0 to 3.5. All the experiments were carried out in triplicate. The HCl and NaOH solutions were previously standardized against primary standards. To calculate the acidity constant (p*K*a) values for the bacterial cells and the corresponding total concentration of the binding sites, data from four replicates of each titration curve were fitted using the program Protofit 2.1 rev1.[2] Variations in the experimental results are reported as the average ± standard derivation.

1.3. Eu^{III} biosorption experiments

S. bentonitica cells were collected at the exponential phase of growth by centrifugation (10000 x g; 10 min). The resultant pellet was washed three times with 0.1 M $NaClO_4$ and resuspended therein to obtain a final biomass concentration of 0.2 g/L. Then, the samples were contacted with 30 µM Eu^{III} solution and incubated at 120 rpm on a rotator shaker at room temperature. The Eu^{III}-bacteria suspensions were harvested by centrifugation (10000 x g; 10 min) after different incubation times (0, 0.5, 1, 2, 24 and 96 h for aerobic and 0, 1, 2, 18, 24 and 48 h for anaerobic experiments). Subsequently, 1 mL of the resultant supernatant was mixed with HNO_3 and measured by inductively coupled plasma mass spectrometry (ICP-MS) to estimate the Eu^{III} concentration. The amount of Eu^{III} adsorbed to the cells was calculated by subtracting the amount obtained in the supernatant from the initial Eu^{III} concentration. For the Eu^{III}-bacteria interaction

under anaerobic conditions the samples were contacted with Eu^{III} under nitrogen atmosphere within a glove box. Eu^{III} solution (30 µM) without addition of cells was employed as control. All samples were performed in triplicate.

1.4. TRLFS experimental setup.

TRLFS studies were performed as described in Moll et al.[3] The Eu^{III}/Cm^{III} single luminescence emission spectra were recorded in the 570–650 nm (1200 line mm^{-1} grating with 0.2 nm resolution) range. The time-dependent luminescence spectra were detected in the 500–700 nm (300 line mm^{-1} grating: high intensity with a lower resolution >0.6 nm) range. For Eu^{III} an excitation wavelength of 394 nm was used. Due to the high absorption of the F-band usually observed in Cm^{3+} excitation spectra, an excitation wavelength of 396 nm was used. For time-dependent Cm emission decay measurements, the delay time between laser pulse and camera gating was scanned with time intervals between 10 and 25 µs. For Eu^{III} a dynamic step width was used to describe species with a long emission life-time as well as species with short emission life time. The following formula was used:

$$t_{\_i} = t_{\_0} + F_{\_1} + F_{\_2} \cdot x \qquad [1]$$

$t_{\_0}$	initial delay, set to 1 µs
$F_{\_1}$	factor 1, set to 5 µs
$F_{\_2}$	factor 2, set to 1 µs
i	number of spectrum
x	number of previous spectrum

The abatement of the luminescence was investigated over at least 40 time points, meaning 40 spectra. The spectra of individual samples were averaged, base-lined and

energy corrected as well as normalized using the ORIGIN 8.6G (OriginLab Corporation, USA) code. The lifetime of luminescent species was obtained also with this software. The Eu^{III} spectra were normalized to the area of the $^7F_1$ band of Eu^{III}.

The relative peak intensity ratio, which gives information about the ligand field of Eu^{III} and the coordination environment, was determined by forming the ratio for the integral intensities of the $^7F_2$ to $^7F_1$ band, as presented in Equation 2:

$$R_{E/M} = (^5D_0 \rightarrow {}^7F_2) / (^5D_0 \rightarrow {}^7F_1) \quad [2]$$

The intensities of I ($^5D_0 \rightarrow {}^7F_2$) and I ($^5D_0 \rightarrow {}^7F_1$) were calculated from the corresponding normalized peak areas. The number of coordinated water molecules was determined based on the equations of Kimura and colleagues,[4–6] which is presented in Equation 3 and 4:

$$nH_2O = 1.07\ k_{exp} - 0.62 \text{ for } Eu^{III} \quad [3]$$

$$nH_2O = 0.65\ k_{exp} - 0.88 \text{ for } Cm^{III} \quad [4]$$

nH_2O = coordination number of water molecules

k_{exp} = reciprocal luminescence emission lifetime (ms)

The spectra deconvolutions of the pH-dependent Cm^{III} luminescence measurements were performed using the factor analysis software HypSpec.[7]

TRLFS is a powerful technique for the direct identification of certain actinide and/or lanthanide complexes resulting from various biogeochemical processes. Luminescent

metal ions emit luminescence light (→ emission spectra) and time-resolved measurements enables to measure the luminescence decay behavior (→ luminescence lifetimes) of excited metal species after irradiated with laser pulses)[8]. This luminescence phenomenon occurs because of their transition from electronically excited states to the ground state. Each type of complex shows ideally a defined luminescence emission spectrum and a certain lifetime and consequently, the analysis of the lifetimes allows the identification of different chemical species produced of a luminescent metal ion.[8] The following images taken from Moll et al. 2020 illustrate the method for a better understanding:

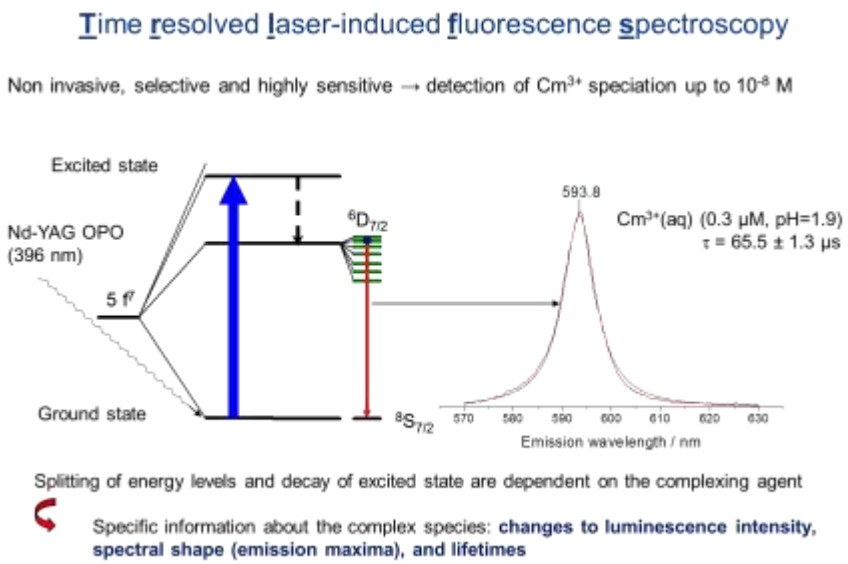

Schema to illustrate the Cm(III) luminescence process (taken from Moll et al. 2020)

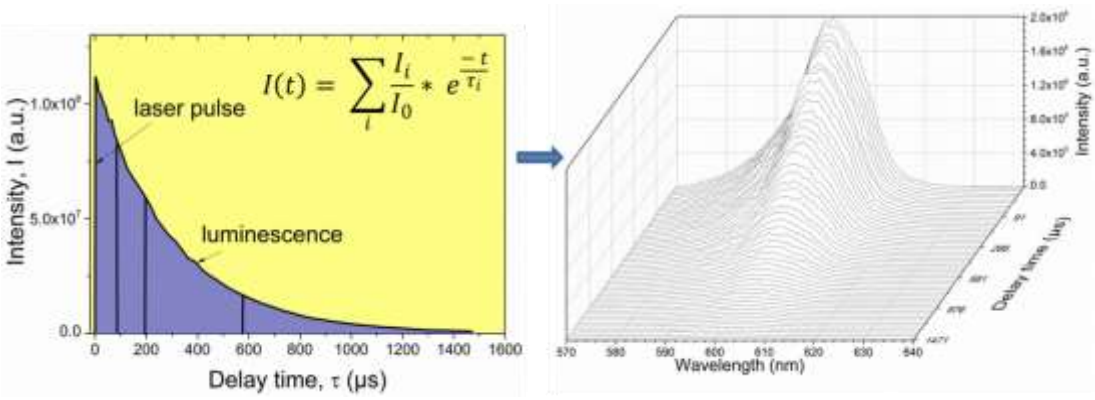

Principal schema of a time-resolved luminescence measurement (sample: 0.88 µM Cm(III), 5 g/l desalted S-layer protein, 0.1 M NaCl, pH 4.0) [taken from Moll et al. 2020].

1.5. STEM-HAADF analysis

The cellular location of Eu^{III} was analyzed by using scanning transmission electron microscopy (STEM) equipped with energy dispersive X-ray (EDX) for elemental composition analysis. EDX analysis was performed at 300 kV using a spot size of 4 Å and a live counting time of 50 s. The samples consisting of Eu^{III}-treated cells (30 µM) under aerobic and anaerobic conditions were prepared as described in Merroun et al.[9] after 48 h of incubation. Finally, the samples were examined under high-angle annular dark field scanning transmission electron microscope (HAADF-STEM) FEI TITAN G2 80-300. STEM specimen holders were cleaned by plasma prior to STEM analysis to minimize contamination.

2. Supplementary figures and tables

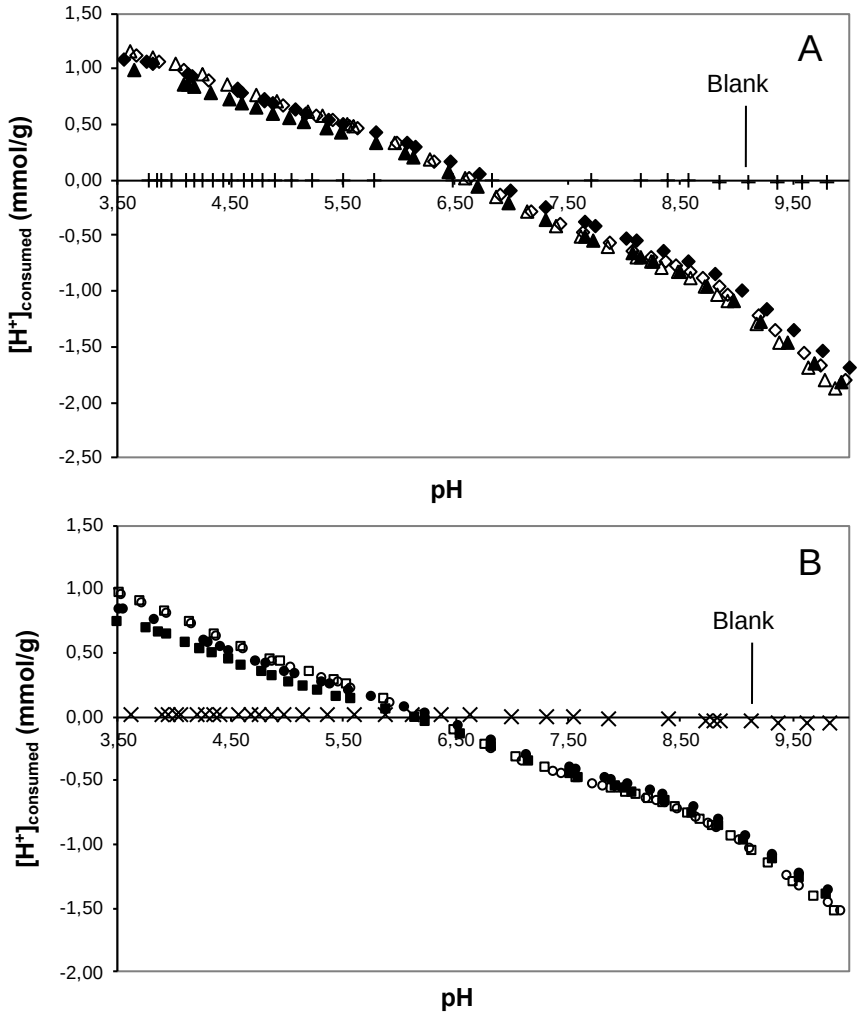

Figure S1. Representation of the potentiometric titrations of *S. bentonitica* in 0.1 M $NaClO_4$ suspension (A) and in contact with 30 µM Eu^{III} solution (B) after 48 hours of incubation, compared with the background electrolyte. Closed symbols correspond to the forward titration data and open symbols correspond to back titration.

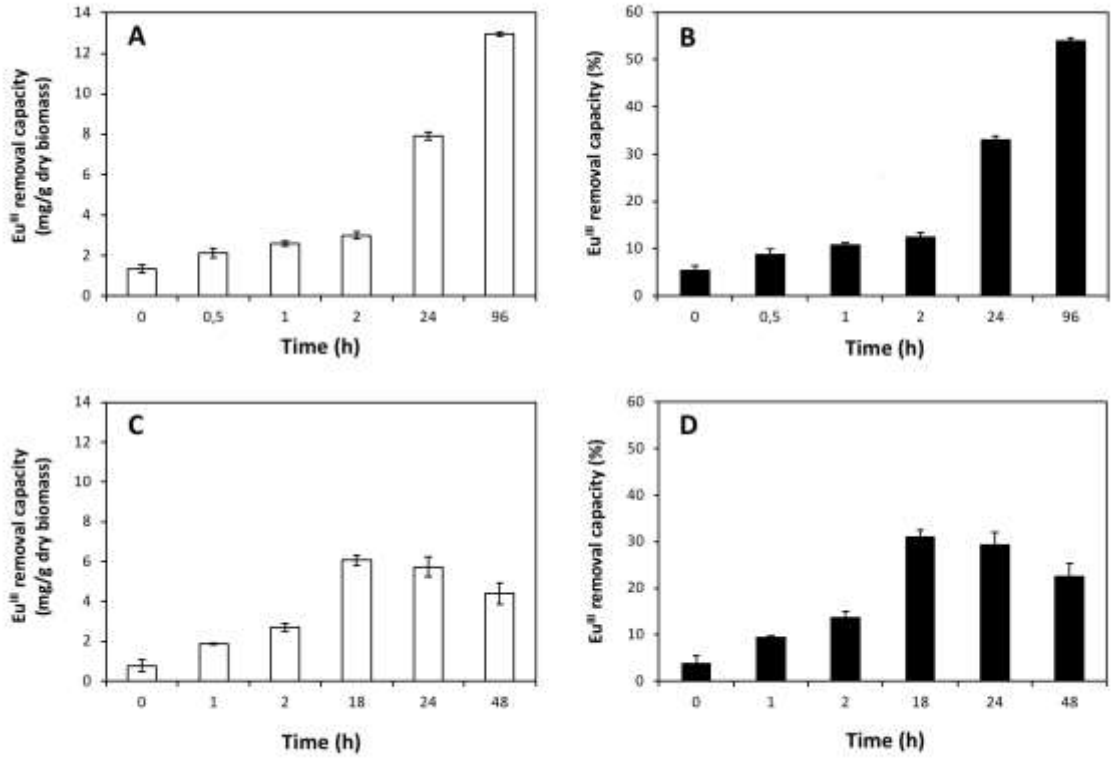

Figure S2. Time dependence in the Eu^{III} removal capacity of *S. bentonitica* cells under aerobic (A and B) and anaerobic (C and D) conditions. The Eu^{III} removal is expressed as mg of Eu per g of dry biomass (A and B) and percentage (B and D).

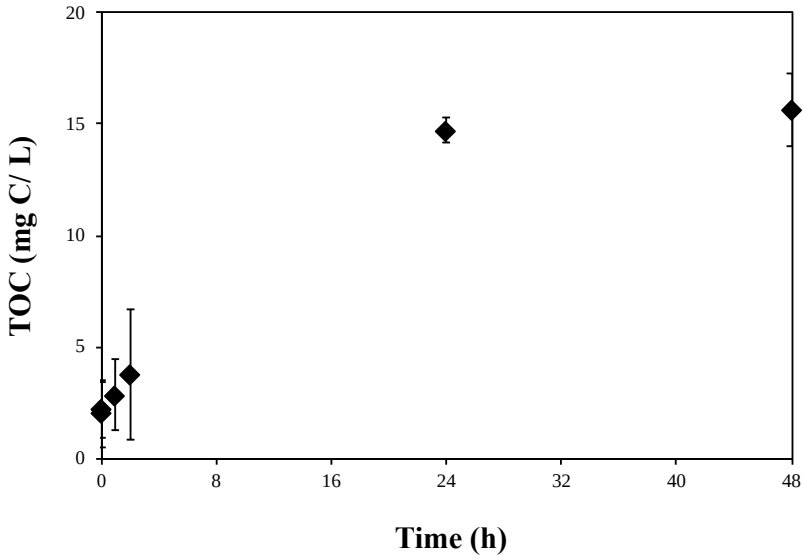

Figure S3. Total organic carbon as a function of time of supernatants obtained after Eu^{III}-*S. bentonitica* interaction under anaerobic conditions.

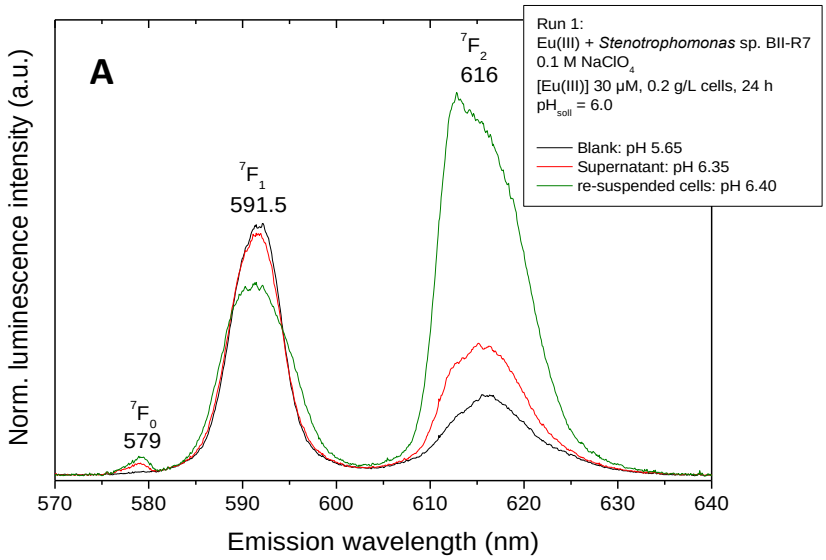

B

Sample	$R_{E/M}$	Lifetime (µs)	Proposed species	Reference
Eu(III) control	0.495	111.5	Eu^{3+}	This work
Supernatants				This work
Eu(III)-*S. bentonitica*				
24 h incubation	0.822	126; 529	Carboxyl; phosphoryl	
Cells				This work
Eu(III)-*S.bentonitica*				
24 h incubation	2.324	207; 516	Carboxyl; phosphoryl	This work

Figure S4. Luminescence emission spectra of 30 µM Eu^{III} measured for the supernatants after separating the *S. bentonitica* cells (0.2 g/L) and the re-suspended cells under aerobic conditions at pH 6 and 24 h incubation in 1 M $NaClO_4$ (A). Spectroscopic properties obtained from the Eu^{III}-*S. bentonitica* system (B).

Table S1. Comparison of deprotonation constants and surface site concentrations for *S. bentonitica* and other strains from different studies.

Species	pK_1	pK_2	pK_3	C_1 (x 10^{-4} mol/g)	C_2 (x 10^{-4} mol/g)	C_3 (x 10^{-4} mol/g)	Model[a]	Reference
S. bentonitica + Electrolyte solution	4.97 ± 0.08	6.88 ± 0.02	9.43± 0.02	5.05 ± 0.31	10.78 ± 0.31	16.93 ± 1.45	NEM	This study
S. bentonitica + Eu(III) solution	4.78 ± 0.06	6.75 ± 0.13	9.48 ± 0.11	5.31 ± 0.22	7.56 ± 0.56	13.99 ± 1.12	NEM	This study
Aquabacterium commune, Gram-negative	3.5 ± 0.8	5.7 ± 0.9	9.1 ± 1.6	4.6 ± 1.5	1.9 ± 0.6	7.3 ± 3.1	NEM	Ojeda et al.[10]
B. sphaericus JG-7B, Gram-positive	4.37 ± 0.27	6.37 ± 0.31	9.95 ± 0.16	4.70 ± 0.55	2.19 ± 0.25	4.56 ± 0.77	NEM	Merroun et al.[11]
Sphingomonas sp. S15-S1, Gram-negative	4.27 ± 0.45	7.03 ± 0.86	9.92 ± 0.32	4.91 ± 1.04	3.16 ± 0.56	9.24 ± 2.97	NEM	Merroun et al.[11]
Enterobacteriaceae, Gram-negative	4.3 ± 0.2	6.9 ± 0.5	8.9 ± 0.5	5.0 ± 0.7	2.2 ± 0.6	5.5 ± 2.2	CCM	Ngwenya et al.[12]
Synechococcus Green, Gram-negative	4.85 ± 0.31	6.56 ± 0.2	8.76 ± 0.06	2.6 ± 0.4	1.9 ± 0.5	2.5 ± 0.4	CCM	Dittrich and Sibler[13]
Synechococcus Red, Gram-negative	4.98 ± 0.16	6.69 ± 0.39	8.66 ± 0.21	7.4 ± 1.6	4.4 ± 0.8	4.8 ± 0.8	CCM	Dittrich and Sibler[13]
Calothrix sp., Gram-negative	4.7 ± 0.4	6.6 ± 0.2	9.1 ± 0.3	3.28 ± 0.27	4.14 ± 0.31	7.16 ± 0.97	NEM	Yee et al.[14]
S. putrefaciens, Gram-negative	5.16 ± 0.04	7.22 ± 0.15	10.04 ± 0.67	0.32 ± 0.02	0.09 ± 0.01	0.38 ± 0.01	CCM	Haas et al.[15]
B. subtilis, Gram-positive	4.8 ± 0.14	6.9 ± 0.5	9.4 ± 0.6	12 ± 1	4.4 ± 0.2	6.2 ± 0.2	CCM	Fein et al.[16]
Sporomusa sp. MT-2.99, Gram-positive	4.8 ± 0.06	6.68 ± 0.06	9.01 ± 0.08	5.3 ± 0.8	3.5 ±0.3	4.8 ± 0.5	-	Moll et al.[17]

[a] CCM = Constant Capacitance Model; NEM = Non-electrostatic model

Table S2. Main infrared absorption bands of the bacterial cell functional groups.[10,13,14,18–20]

Wavenumber (cm^{-1})	**Functional group assignment**
1745	Stretching C=O of ester functional groups from membrane lipids and fatty acids; stretching C=O of carboxylic acids.
1635	Stretching C=O in amides (amide I band)
1531	N-H bending and C-N stretching in amides (amide II band). Asymmetric stretching for deprotonated COO^- groups.
1404	Symmetric stretching for deprotonated COO^- group.
1455	Bending CH_2/CH_3 (scissoring)
1308	Bending CH_2/CH_3
1300-1250	Vibrations of C-O from esters or carboxylic acids
1240	Vibrations of -COOH and C-O-H; Double bond stretching of >P=O of general phosphoryl groups and phosphodiester of nucleic acids.
1225	Stretching of P=O in phosphates.
1200-950	Asymmetric and symmetric stretching of PO_2^- and $P(OH)_2$ in phosphates; vibrations of C-OH, C-O-C and C-C of polysaccharides.
1070	Stretching P=O of phosphodiester, phosphorilated proteins or polyphosphate products.
933	Symmetric stretching vibration of phosphoryl groups.

Table S3. Luminescence emission data of the Cm^{III}-*S. bentonitica* system including those of relevant model systems for comparison.

Species	Emission peak maximum (nm)	Lifetime (µs)	Reference
Cm^{III} (aq)	593.5	68 ± 5	This work
Cm^{III} -*S.bentonitica* BII-R7 species 1	599.6	290 ± 23	This work
Cm^{III} -*S.bentonitica* BII-R7 species 2	601.1	120 ± 8	This work
Cm^{III} -*R. mucilaginosa* BII-R8 species 1	599.6	240 ± 50	Lopez-Fernandez et al.[1]
Cm^{III} -*R. mucilaginosa* BII-R8 species 2	601.5	123 ± 11	
Cm^{III} -*Sporomusa* sp. MT-2.99 complexes			Moll et al.[17]
R-O-PO_3H-Cm^{2+}	599.8	252 ± 46	
R-COO-Cm^{2+}	601.6	108 ± 15	
Cm^{III} -*Pseudomonas fluorescens* complexes			Moll et al.[21]
R-O-PO_3H-Cm^{2+}	599.6	390 ± 78	
R-COO-Cm^{2+}	601.9	121 ± 10	
Cm^{III} -*Paenibacillus* sp. complex			Lütke[22]
R-O-PO_3H-Cm^{2+}	598.8	477 ± 73	

3. References

(1) Lopez-Fernandez, M.; Moll, H.; Merroun, M. L. Reversible PH-Dependent Curium(III) Biosorption by the Bentonite Yeast Isolate Rhodotorula Mucilaginosa BII-R8. *J. Hazard. Mater.* **2018**. https://doi.org/https://doi.org/10.1016/j.jhazmat.2018.06.054.

(2) Turner, B. F.; Fein, J. B. Protofit: A Program for Determining Surface Protonation Constants from Titration Data. *Comput. Geosci.* **2006**, *32* (9), 1344–1356. https://doi.org/10.1016/j.cageo.2005.12.005.

(3) Moll, H.; Glorius, M.; Barkleit, A.; Rossberg, A.; Bernhard, G. The Mobilization of Actinides by Microbial Ligands Taking into Consideration the Final Storage of Nuclear Waste. **2009**.

(4) Kimura, T.; Choppin, G. R.; Kato, Y.; Yoshida, Z. Determination of the Hydration Number of Cm(III) in Various Aqueous Solutions. *Radiochim. Acta* **1996**. https://doi.org/10.1524/ract.1996.72.2.61.

(5) Kimura, T.; Kato, Y. Luminescence Study on Hydration States of Lanthanide(III)-Polyaminopolycarboxylate Complexes in Aqueous Solution. *J. Alloys Compd.* **1998**. https://doi.org/10.1016/S0925-8388(98)00446-0.

(6) Kimura, T.; Choppin, G. R. Luminescence Study on Determination of the Hydration Number of Cm(III). *J. Alloys Compd.* **1994**. https://doi.org/10.1016/0925-8388(94)90921-0.

(7) Gans, P.; Sabatini, A.; Vacca, A. Investigation of Equilibria in Solution. Determination of Equilibrium Constants with the HYPERQUAD Suite of Programs. *Talanta* **1996**. https://doi.org/10.1016/0039-9140(96)01958-3.

(8) Moll, H.; Lehmann, F.; Raff, J. Interaction of Curium(III) with Surface-Layer Proteins from Lysinibacillus Sphaericus JG-A12. *Colloids Surfaces B Biointerfaces* **2020**. https://doi.org/10.1016/j.colsurfb.2020.110950.

(9) Merroun, M. L.; Raff, J.; Rossberg, A.; Hennig, C.; Reich, T.; Selenska-Pobell, S. Complexation of Uranium by Cells and S-Layer Sheets of Bacillus Sphaericus JG-A12. *Appl. Environ. Microbiol.* **2005**. https://doi.org/10.1128/AEM.71.9.5532-5543.2005.

(10) Ojeda, J. J.; Romero-González, M. E.; Bachmann, R. T.; Edyvean, R. G. J.; Banwart, S. A. Characterization of the Cell Surface and Cell Wall Chemistry of Drinking Water Bacteria by Combining XPS, FTIR Spectroscopy, Modeling, and Potentiometric Titrations. *Langmuir* **2008**, *24* (8), 4032–4040. https://doi.org/10.1021/la702284b.

(11) Merroun, M. L.; Nedelkova, M.; Ojeda, J. J.; Reitz, T.; Fernández, M. L.; Arias, J. M.; Romero-González, M.; Selenska-Pobell, S. Bio-Precipitation of Uranium by Two Bacterial Isolates Recovered from Extreme Environments as Estimated by Potentiometric Titration, TEM and X-Ray Absorption Spectroscopic Analyses. *J. Hazard. Mater.* **2011**, *197*, 1–10. https://doi.org/10.1016/j.jhazmat.2011.09.049.

(12) Ngwenya, B. T.; Sutherland, I. W.; Kennedy, L. Comparison of the Acid-Base Behaviour and Metal Adsorption Characteristics of a Gram-Negative Bacterium with Other Strains. *Appl. Geochemistry* **2003**. https://doi.org/10.1016/S0883-2927(02)00118-X.

(13) Dittrich, M.; Sibler, S. Cell Surface Groups of Two Picocyanobacteria Strains Studied by Zeta Potential Investigations, Potentiometric Titration, and Infrared Spectroscopy. *J. Colloid Interface Sci.* **2005**. https://doi.org/10.1016/j.jcis.2005.01.029.

(14) Yee, N.; Benning, L. G.; Phoenix, V. R.; Ferris, F. G. Characterization of Metal-Cyanobacteria Sorption Reactions: A Combined Macroscopic and Infrared Spectroscopic Investigation. *Environ. Sci. Technol.* **2004**. https://doi.org/10.1021/es0346680.

(15) Haas, J. R.; Dichristina, T. J.; Wade, R. Thermodynamics of U(VI) Sorption onto Shewanella Putrefaciens. *Chem. Geol.* **2001**, *180* (1–4), 33–54. https://doi.org/10.1016/S0009-2541(01)00304-7.

(16) Fein, J. B.; Daughney, C. J.; Yee, N.; Davis, T. A. A Chemical Equilibrium Model for Metal Adsorption onto Bacterial Surfaces. *Geochim. Cosmochim. Acta* **1997**. https://doi.org/10.1016/S0016-7037(97)00166-X.

(17) Moll, H.; Lütke, L.; Bachvarova, V.; Cherkouk, A.; Selenska-Pobell, S.; Bernhard, G. Interactions of the Mont Terri Opalinus Clay Isolate Sporomusa Sp. MT-2.99 with Curium(III) and Europium(III). *Geomicrobiol. J.* **2014**. https://doi.org/10.1080/01490451.2014.889975.

(18) Conley, R. T. Infrared Spectroscopy; Boston., 1972.

(19) Jiang, W.; Saxena, A.; Song, B.; Ward, B. B.; Beveridge, T. J.; Myneni, S. C. B. Elucidation of Functional Groups on Gram-Positive and Gram-Negative Bacterial Surfaces Using Infrared Spectroscopy. *Langmuir* **2004**. https://doi.org/10.1021/la049043+.

(20) Schmitt, J.; Flemming, H. C. FTIR-Spectroscopy in Microbial and Material Analysis. *Int. Biodeterior. Biodegrad.* **1998**. https://doi.org/10.1016/S0964-8305(98)80002-4.

(21) Moll, H.; Lütke, L.; Barkleit, A.; Bernhard, G. Curium(III) Speciation Studies with Cells of a Groundwater Strain of Pseudomonas Fluorescens. *Geomicrobiol. J.* **2013**. https://doi.org/10.1080/01490451.2012.688927.

(22) Lütke, L. Interaction of Selected Actinides (U, Cm) with Bacteria Relevant to Nuclear Waste Disposal. *Dr. thesis TU Dresden, Ger.* **2013**.